New model of axion monodromy inflation and its cosmological implications

Yi-Fu Cai, 1, 2, * Fang Chen, 3, † Elisa G. M. Ferreira, 2, ‡ and Jerome Quintin § 2, ¶

¹CAS Key Laboratory for Researches in Galaxies and Cosmology,
Department of Astronomy, University of Science and Technology of China,
Chinese Academy of Sciences, Hefei, Anhui 230026, China
²Department of Physics, McGill University, Montréal, QC, H3A 2T8, Canada
³Kavli Institute for Theoretical Physics, University of California, Santa Barbara, California 93106, USA

We propose a new realization of axion monodromy inflation in which axion monodromy arises from torsional cycles in a type IIB compactification. A class of monomial potentials is obtained with specific values for the power index. Moreover, the inflaton mass changes profile due to the couplings between various fields after compactification. Consequently, the potential obtains a step-like profile at some critical scale. We study the cosmological implications of one concrete realization of this model. At the background level, it realizes a sufficiently long inflationary stage, which allows for the violation of the slow-roll conditions for a short period of time when the inflaton is close to the critical scale. Accordingly, the Hubble horizon is perturbed and affects the dynamics of primordial cosmological perturbations. In particular, we analyze the angular power spectrum of B-mode polarization and find a boost on very large scales. We also find that the amplitude of scalar perturbations is suppressed near the critical scale. Thus our model provides an interpretation for the low- ℓ suppression of temperature anisotropies in the CMB power spectrum. We examine these effects and confront the model to observations.

PACS numbers: 98.80.Cq, 98.80.Es, 11.25.Mj

I. INTRODUCTION

Large field inflationary models with super-Planckian field ranges are observationally allowed by the latest cosmological experiments [1, 2]. The recent detection of primordial B-mode polarization reported by the BICEP2 experiment implies that the tensor-to-scalar ratio, r, which is the ratio between the amplitude of the spectra of tensor and scalar perturbations, is likely to be nonzero [3]. This favors models of large field inflation via the Lyth bound [4]. While the understanding of the BICEP2 data in terms of primordial tensor fluctuations becomes less clear [5, 6] because of a potential contamination by the dust foreground detected by the Planck group [7], it remains of theoretical interests to study the realization of large field inflation within the framework of fundamental particle physics.

Considering the fact that inflation could occur near the Grand Unified Theory (GUT) scale, it is natural to ask whether large field inflation can be realized within string theory. In the literature, this topic has received extensive attention (for instance, see [8–10] for recent reviews). Recently, it was put forward and analyzed in [11–13] that a string theory model of large field inflation can be achieved under the axion monodromy construction. In the corresponding stringy setup, a number of axion fields coupled to fluxes can yield a super-Planckian field

variation while softly breaking the shift symmetry along the axion potential due to the coupling or due to D-branes. As a result, a class of axion monodromy inflation models with monomial potentials was obtained in [14]. Various extended analyses of axion monodromy inflation were performed in the literature, for instance, in the context of super-gravity (SUGRA) realizations [15–17], by involving extra moduli fields [18, 19], or by making connections to natural inflation [20–24]. Also, a potential back-reaction issue against the moduli stabilization was recently discussed in [25–27] from different perspectives.

In the present paper, we propose a new realization of axion monodromy inflation in terms of a set of D3- and D5-branes with torsional cycles. Our model represents a formulation of inflation from a class of string theory models presented in [15]. In our concrete construction, the potential for the inflaton field approximately takes the form of a power law function in which the exponent (p) varies depending on the detailed integral over the internal manifold as well as on the contribution from a Chern-Simons term. In general, these functions can appear as a linear combination in a single potential, which can be expressed as

$$V(\varphi) = \sum_{i} c_i \varphi^{p_i} ,$$

where the c_i 's are to be determined by the specific constructions. Therefore, our model can easily give rise to a sufficiently long period of inflation that is required by cosmological observations. More interestingly, we take a closer look at the shape of the inflaton's potential and we find that it may receive a modulation due to the uncertainty in the integration of the internal space. As a result, we expect this nontrivial modulation in the potential to leave important signals for cosmological experiments.

[§]Vanier Canada Graduate Scholar.

^{*}Electronic address: yifucai@ustc.edu.cn

[†]Electronic address: fchen@kitp.ucsb.edu

[‡]Electronic address: elisafenu@physics.mcgill.ca

 $[\]P$ Electronic address: jquintin@physics.mcgill.ca

As a representative example, we study a specific inflation model derived from our construction. In particular, we analyze a model of chaotic inflation with a potential of the form $m^2\varphi^2$ in which the inflaton mass obtains a small modulation due to the variation of the internal space. Therefore, the inflaton potential possesses a steplike feature at a critical scale φ_c . We study in detail the cosmological implications of this model and we find that the mass modulation leads to a short phase of slow-roll violation during inflation when the inflaton field approaches φ_c . The Hubble horizon near the corresponding scale is also perturbed due to the violation of the slow-roll conditions. Accordingly, for the primordial fluctuations exiting the Hubble horizon at the same moment, the process of getting squeezed can be dramatically affected. In general, the spectrum of these fluctuation modes can become wiggly, but if the modulation is smooth enough, the spectrum can present a suppression behavior near the critical scale and then grow back to a larger amplitude at even larger length scales. We analyze these effects in the primordial angular power spectrum of temperature anisotropies and confront them with the Planck 2013 data. Our results show that, for certain values of the model parameters, an appropriate suppression of the power can be achieved to explain the cosmic microwave background (CMB) anomaly at large angular scales. We further study the angular power spectrum of B-mode polarization that arises from primordial gravitational waves and obtain a small enhancement on very large scales. While being aware of the fact that the amplitude of primordial tensor fluctuations can always be modified by tuning the inflationary model parameters, the small amplification feature in the B-mode spectrum is a key prediction made by our model. This particular prediction may shed light on probing new physics by virtue of accumulating high-precision CMB polarization data in the near future.

The paper is organized as follows. In Sec. II, we first briefly review the general picture of axion monodromy inflation and then propose a new realization for axion monodromy inflation in string theory. Afterwards, we select a specific realization of our new axion monodromy model in Sec. III and we study its cosmological implications in detail. We first study the background inflationary solution and analyze the dynamics of the slow-roll parameters. Then we numerically calculate the primordial power spectra of scalar and tensor perturbations generated during inflation. We then confront the theoretical predictions of our specific model with the latest CMB data by analyzing the temperature and B-mode polarization angular power spectra, and we perform Markov Chain Monte Carlo (MCMC) simulations to constrain the model. We conclude with a discussion in Sec. IV. Throughout this paper, we adopt the convention $M_p^2 \equiv 1/8\pi G$.

II. A MODEL OF AXION MONODROMY INFLATION

In this section we first present a brief review of the regular version of axion monodromy inflation and then propose a new model in the presence of torsional cycles.

A. A brief review of existing axion monodromy models

The idea of axion monodromy inflation originally proposed in [11] has provided an interesting interpretation that a sufficiently long period of inflation can persist through many cycles of the axion period while the inflaton's potential is well controlled by the axion shift symmetry. This model, and related extensions, were widely studied since then (see, e.g., [12, 13, 15, 28–33] and references therein).

In most of these models, the axion field comes from the reduction of a NS-NS two-form B_2 on a two-cycle which has a continuous shift symmetry due to the higher dimensional gauge symmetry of the two-form, and the monodromy is induced by branes or fluxes. As a simple example, one can consider a D5-brane wrapping an internal two-cycle Σ_2 in type IIB string theory. The axion, which is given by $b=\frac{1}{\alpha'}\int_{\Sigma_2}B_2$, has a shift symmetry $b\to b+{\rm const.}$ However, the presence of the D5-brane gently breaks such a shift symmetry and generates the monodromy. To be explicit, we can consider the Dirac-Born-Infeld (DBI) action for the D5-brane,

$$S_{D5} = \frac{1}{(2\pi)^5 g_s \alpha'^3} \int_{\mathcal{M}_4 \times \Sigma_2} d^6 x \sqrt{-\det(G_{ab} + B_{ab})} , (1)$$

which is an effective field description of string theory at low energy scales. Here, \mathcal{M}_4 denotes the 3+1 space-time, and G_{ab} and B_{ab} , where a, b = 0, ..., 5, are the induced metric and NS-NS two-form on the D5-brane world volume, respectively.

After integrating over the two-cycle Σ_2 , one obtains the potential of the axion in the four-dimensional effective theory,

$$V(b) = \frac{\rho}{(2\pi)^6 g_s \alpha^2} \sqrt{(2\pi)^2 \ell^4 + b^2} , \qquad (2)$$

where ℓ is the size of the two-cycle Σ_2 in string units and ρ is a dimensionless coefficient determined by the warp factor. For large values of b, the potential is linear, $V(b) \propto b$. Correspondingly, the Lagrangian of the canonically normalized inflaton field φ is given by,

$$\mathcal{L} = -\frac{1}{2}(\partial\varphi)^2 - m^3\varphi, \text{ with } m^3 = \frac{1}{f}\frac{\rho}{(2\pi)^6 g_s \alpha'^2}, \quad (3)$$

where f is the axion decay constant. In addition, a similar scenario can be achieved when the D5-brane is replaced by an NS5-brane.

It has been interestingly observed that there are many variants of the axion's potential that may arise from axion monodromy. Thus, it is convenient to parameterize these theories in terms of an exponent p:

$$\mathcal{L} = -\frac{1}{2}(\partial\varphi)^2 - m^{4-p}\varphi^p \ . \tag{4}$$

For example, a model with p=2/3 was obtained in [11] based on a construction of Nil manifolds; the case of p=2 was found after taking into account an appropriate coupling of the axion to a four-form field [34]; more examples with p=2/3, 4/3, 2 and 3 were obtained in [14] by considering effective couplings of the NS-NS B_2 field to the RR F_1 field through $|\tilde{F}_5|^2$ and $|\tilde{F}_3|^2$, respectively, after reducing type IIB on a circle with specific background fluxes and moduli stabilization.

Another interesting model of axion monodromy inflation was constructed in [15], where the axion arises from the KK compactification of higher dimensional gauge fields or p-form potentials in the presence of fluxes and/or torsion homology. The presence of these extra components generate the F-term potential. In the same work the authors argued that this scenario could naturally avoid the η -problem widely existing in the inflationary paradigm [35] since those axions did not appear in the Kähler potential as they did in other models.

B. New axion monodromy inflation from warped torsion classes

We propose a new model of axion monodromy inflation in the present subsection. This represents a realization from a class of axion monodromy models where the F-term potential comes from the inclusion of extra ingredients, as seen in [15]. In our model we include torsional cycles. Specifically, we consider a type IIB string theory compactification and assume that there are N D3-branes along the 3+1 space-time. Thus the metric naturally has a warp factor $e^{-2A} \sim 1/N$, maintaining the four-dimensional Poincaré invariance, and takes the form

$$ds_{10}^2 = e^{-2A(y^i)} dx_\mu dx^\mu + e^{2A(y^i)} dy_i dy^i , \qquad (5)$$

where $\mu = 1, ..., 4$ represents the coordinates of the physical space-time, and i = 1, ..., 6 runs over the coordinates of the internal manifold \mathcal{M}_6 .

It is well known that in a (conformal) Calabi-Yau (CY) compactification, the massless modes are in one-to-one correspondence with elements of the cohomology groups of the internal manifold, modulo certain subtleties that arise once one introduces warping [36–42]. However, the situation becomes slightly different if there are torsional cycles since in this case, the massless modes are not sensitive to D-branes wrapping torsional cycles. In the following we use X_6 to denote the unwarped internal manifold and distinguish it from \mathcal{M}_6 . In general, there are two independent torsion classes in a six-dimensional

manifold, i.e., torsion one-cycles Σ_1 and torsion two-cycles Σ_2 . They can be related to torsion four-cycles Σ_4 and torsion three-cycles Σ_3 via

$$\operatorname{Tor} H_r(X_d, \mathbb{Z}) = \operatorname{Tor} H_{d-r-1}(X_d, \mathbb{Z}) ,$$
 (6)

for a d-dimensional internal manifold and any positive integer r. For simplicity we take

$$\operatorname{Tor} H_1(X_6, \mathbb{Z}) = \operatorname{Tor} H_4(X_6, \mathbb{Z}) = \mathbb{Z}_p$$

$$\operatorname{Tor} H_2(X_6, \mathbb{Z}) = \operatorname{Tor} H_3(X_6, \mathbb{Z}) = \mathbb{Z}_k , \qquad (7)$$

where p and k are positive integers and in general not equal. Now let us consider a set of non-harmonic Laplacian eigenforms of X_6 ,

$$d\gamma_1 = p\rho_2 , d\tilde{\rho}_4 = p\tilde{\gamma}_5 , \qquad (8)$$

$$d\eta_2 = k\omega_3 \ , \ d\tilde{\omega}_3 = k\tilde{\eta}_4 \ , \tag{9}$$

where γ_1 , $\tilde{\rho}_4$, η_2 , and $\tilde{\omega}_3$ are associated with the generators of $\operatorname{Tor} H_i(X_6,\mathbb{Z})$ with $i=1,\,4,\,2$, and 3, respectively. We note that, ρ_2 , $\tilde{\gamma}_5$, ω_3 , and $\tilde{\eta}_4$ are trivial in de Rham cohomology but are non-trivial generators of $H^i(X_6,\mathbb{Z})$, i=2,5,3,4. Additionally, we have the following integral constraints:

$$\int \gamma_1 \wedge \tilde{\gamma}_5 = \int \rho_2 \wedge \tilde{\rho}_4 = \int \eta_2 \wedge \tilde{\eta}_4 = \int \tilde{\omega}_3 \wedge \omega_3 = 1.$$
(10)

Then we can expand type IIB NS-NS and RR forms in terms of these eigenforms as

$$B_{2} = b\eta_{2} + \bar{b}\rho_{2} + b_{1} \wedge \gamma_{1} + b_{2} ,$$

$$C_{2} = c\eta_{2} + \bar{c}\rho_{2} + c_{1} \wedge \gamma_{1} + c_{2} ,$$

$$C_{4} = \mathfrak{c}\tilde{\rho}_{4} + \bar{\mathfrak{c}}\tilde{\eta}_{4} + \mathfrak{c}_{1} \wedge \tilde{\omega}_{3} + \bar{\mathfrak{c}}_{1} \wedge \omega_{3} + \mathfrak{c}_{2} \wedge \rho_{2} + \bar{\mathfrak{c}}_{2} \wedge \eta_{2} + \mathfrak{c}_{3} \wedge \gamma_{1} + \mathfrak{c}_{4} ,$$

$$(11)$$

and they are the most general expansions regardless of the orientation. The corresponding ten-dimensional field strengths are given by

$$H_{3} \equiv dB_{2} = db \wedge d\eta_{2} + kb\omega_{3} + (d\bar{b} - pb_{1}) \wedge \rho_{2}$$

$$+ db_{1} \wedge \gamma_{1} + db_{2} ,$$

$$F_{3} \equiv dC_{2} = dc \wedge d\eta_{2} + kc\omega_{3} + (d\bar{c} - pc_{1}) \wedge \rho_{2}$$

$$+ dc_{1} \wedge \gamma_{1} + dc_{2} ,$$

$$F_{5} \equiv dC_{4} = d\mathbf{c} \wedge \tilde{\rho}_{4} + p\mathbf{c}\tilde{\gamma}_{5} + (d\bar{\mathbf{c}} - k\mathbf{c}_{1}) \wedge \tilde{\eta}_{4} + d\mathbf{c}_{1} \wedge \tilde{\omega}_{3}$$

$$+ (d\bar{\mathbf{c}}_{1} + k\bar{\mathbf{c}}_{2}) \wedge \omega_{3} + (d\mathbf{c}_{2} - p\mathbf{c}_{3}) \wedge \rho_{2}$$

$$+ d\bar{\mathbf{c}}_{2} \wedge \eta_{2} + d\mathbf{c}_{3} \wedge \gamma_{1} + d\mathbf{c}_{4} . \tag{12}$$

Next, we perform the dimensional reduction of the type IIB SUGRA action on \mathcal{M}_6 . The type IIB SUGRA action including local sources in ten dimensions is then given by

$$S = \frac{1}{2\kappa_{10}^2} \int d^{10}x \sqrt{G} \left(R + \frac{\partial_M \tau \partial^M \bar{\tau}}{2|\text{Im}\tau|^2} - \frac{|\tilde{F}_5|^2}{4 \cdot 5!} - \frac{G_3 \cdot \bar{G}_3}{12\text{Im}\tau} \right) + \frac{1}{8i\kappa_{10}^2} \int \frac{C_4 \wedge G_3 \wedge \bar{G}_3}{\text{Im}\tau} + S_{\text{loc}}$$
(13)

in Einstein frame, where $\tau = C_0 + ie^{-\phi}$ is the axiondilaton field with C_0 being the string axion (one should be aware that this is not the same axion field as the one we will discuss below in the four-dimensional effective theory) and ϕ being the dilation field. Moreover,

$$\tilde{F}_5 = dC_4 - \frac{1}{2}C_2 \wedge H_3 + \frac{1}{2}B_2 \wedge F_3 ,$$
 (14)

which is the five-form flux, and

$$G_3 = F_3 - \tau H_3 \ , \tag{15}$$

with F_3 being the RR three-form flux and H_3 the NS-NS three-form flux. Also, G is the determinant of the tendimensional metric g_{MN} , where M, N = 0, ..., 9. Finally, S_{loc} is the action for localized sources in the system, i.e. D3-branes in our case.

The presence of this finite number of localized D3-branes leads to the appearance of a D3-brane charge density. Integrating the Bianchi identity (or equation of motion) for the five-form flux over X_6 , we arrive at the tadpole cancellation condition,

$$Q_3^{\text{loc}} + \frac{1}{2\kappa^2 T_3} \int_{X_6} H_3 \wedge F_3 = 0 ,$$
 (16)

where $Q_3^{\rm loc}$ is the charge associated with the D3-brane. The charge must be conserved so that the tadpole condition is not violated. Here, the presence of the N D3-branes leads to the presence of D3-brane charges since at every axion period the B-fields induce these charges. To solve this problem, we propose the inclusion of 3-form fluxes. Those fluxes carry the amount of D3-brane charge given by the integral in (16). So, by a suitable choice of fluxes, the tadpole condition can be met. Another consequence is that their inclusion is responsible for stabilizing the complex structure and the dilaton moduli. We comment in the next subsection in more detail about the inclusion of those fluxes and about the moduli stabilization issue.

Plugging Eq. (11) and Eq. (12) into Eq. (13) gives rise to the four-dimensional effective action that we are interested in. In particular, we are mostly interested in the contributions from the scalar fields b, c and \mathfrak{c} , and hence, the effective action in four dimensions can be simplified as

$$S_{4} = -\int d^{4}x \, \frac{\sqrt{g_{4}}}{24\kappa_{10}^{2}} \Big[(\mathcal{T}_{1} + \mathcal{T}_{2}c^{2})\partial_{\mu}b\partial^{\mu}b$$

$$+ (\mathcal{T}_{1} + \mathcal{T}_{2}b^{2})\partial_{\mu}c\partial^{\mu}c + k^{2}\mathcal{T}_{3}(b^{2} + c^{2})$$

$$+ \mathcal{T}_{2}bc \, \partial_{\mu}b\partial^{\mu}c + \mathcal{T}_{4}\partial_{\mu}\mathfrak{c}\partial^{\mu}\mathfrak{c} + p^{2}\mathcal{T}_{5}\mathfrak{c}^{2} \Big]$$

$$+ \dots , \qquad (17)$$

where

$$\mathcal{T}_{1} = \int \eta_{2} \wedge \star_{6} \eta_{2}, \quad \mathcal{T}_{2} = \int e^{-4A} \, \eta_{2} \wedge \eta_{2} \wedge \star_{6} (\eta_{2} \wedge \eta_{2}),$$

$$\mathcal{T}_{3} = \int e^{-4A} \, \omega_{3} \wedge \star_{6} \omega, \quad \mathcal{T}_{4} = \int e^{-4A} \, \tilde{\rho}_{4} \wedge \star_{6} \tilde{\rho}_{4},$$

$$\mathcal{T}_{5} = \int e^{-8A} \, \tilde{\gamma}_{5} \wedge \star_{6} \tilde{\gamma}_{5}.$$
(18)

Also, g_4 is the determinant of the unwarped space-time metric and the hodge star \star_6 is associated with the unwarped internal manifold X_6 . In the above, we have set the axion C_0 and dilaton ϕ to zero. We also work only at leading order in α' ; at higher orders in α' , there will perturbative corrections to the kinetic terms, as studied for example in [43], in addition to the usual curvature corrections¹. The ellipsis at the end of the action denotes the contributions from the ten-dimensional Chern-Simons term and other relevant terms, which are all linear in the b, c, and $\mathfrak c$ fields.

To normalize the b field, we introduce

$$\mathfrak{b} = \frac{\kappa_4 \sqrt{\mathcal{T}_1 + \mathcal{T}_2 c^2}}{2\sqrt{3}\kappa_{10}} b . \tag{19}$$

Thus the b- and c-related terms in the action can be written as

$$S_4 \sim -\int d^4x \, \frac{\sqrt{g_4}}{2\kappa_4^2} \Big[\partial_\mu \mathfrak{b} \partial^\mu \mathfrak{b} + \frac{k^2 \mathcal{T}_3}{\mathcal{T}_1 + \mathcal{T}_2 c^2} \mathfrak{b}^2 + (\mathcal{T}_1 + \mathcal{T}_2 b^2(\mathfrak{b})) \partial_\mu \tilde{c} \partial^\mu \tilde{c} + k^2 \mathcal{T}_3 \tilde{c}^2 \Big] , \qquad (20)$$

where $\tilde{c} = \kappa_4 c / (2\sqrt{3}\kappa_{10})$.

The above three scalar fields \mathfrak{b} , c (or \tilde{c} equivalently), and \mathfrak{c} can be candidates for the inflation field. On one hand, as has been argued in [15], in the (conformal) CY compactification the b field is generally involved in the Kähler potential. Thus, if one takes the \mathfrak{b} field as the inflaton field, upon the moduli stabilization, the corresponding potential could achieve a correction that renders a possibly large value of the η parameter ($\eta \sim 1$), and therefore may invalidate the occurrence of inflation. On the other hand, the \mathfrak{c} field gives rise to the standard chaotic inflation by checking the last two terms of the action (17). We also note that the \mathfrak{c} field is decoupled from the other two fields. Therefore, we focus on the cosmological implications of the \tilde{c} field.

Before we study the inflaton field, we also have to stabilize the $\mathfrak b$ field. We notice that the $\mathfrak b$ field couples to the c field in a non-standard way and that the value $\mathfrak b_{\min}$ where its potential is the lowest depends on c. Since we know that $e^{-4A} \sim 1/N^2$, the c dependence is mild if $c < N^2$ and strong if $c > N^2$. In particular, for $c < N^2$ we ignore its dependence in the $\mathfrak b$ potential and $\mathfrak b_{\min}$ is fixed; for $c > N^2$ we will see that it can give rise to cosmological inflation. Thus, we can set $c = N^2$ temporarily in order to find $\mathfrak b_{\min}$ in this region.

Now that \mathfrak{b}_{\min} is fixed, b_{\min} can also be determined. Thus we can normalize the c field and write down the

As mentioned below equation (5), there are also subtleties that arise once one considers non-small warping. In particular, solving the Einstein equation requires a careful analysis of the 'breathing mode' and the introduction of a compensator field (see, e.g., [42]).

four-dimensional effective action as follows,

$$S_4 = -\frac{1}{2} \int d^4x \, \sqrt{g_4} \Big(\partial_\mu \varphi \partial^\mu \varphi + m^2 \varphi^2 \Big) \,, \qquad (21)$$

where

$$\varphi = \sqrt{\mathcal{T}_1 + \mathcal{T}_2 b_{\min}^2} \,\tilde{c} ,$$

$$m^2 = \frac{k^2}{\mathcal{T}_1 + \mathcal{T}_2 b_{\min}^2} . \tag{22}$$

One could do another field transformation in Eq. (21) to absorb the linear term and leave the mass m^2 unchanged. The resulting cosmological solution would lead to simple chaotic inflation. Instead, we would like to explore another possibility in which the mass of the inflaton field varies along the inflaton value, which occurs at

$$\varphi_c = \frac{\kappa_4 \sqrt{T_1 + T_2 b_{\min}^2(N^2)} N^2}{2\sqrt{3}\kappa_{10}} \ . \tag{23}$$

This can be achieved when the flux coupling, which determines the mass of the inflaton field, varies between the inside and outside of the warped manifold. Such a variation of the flux coupling can lead to a modulation at a critical scale. To see this more explicitly, we rewrite the mass term as follows,

$$m^2\varphi^2 = \left[m_a^2 + (m_b^2 - m_a^2)\theta(\varphi - \varphi_c)\right]\varphi^2 , \qquad (24)$$

where m_a^2 and m_b^2 are the inflaton masses when the inflaton field is smaller and larger than the critical value φ_c , respectively. We have used the θ function here to describe the most extremal case. However, as we discussed previously, $b_{\min}(c)$ is smooth, so instead of the step function θ , it is better to use the following parametrization,

$$m^{2}\varphi^{2} = m_{a}^{2}\varphi^{2} + \frac{(m_{b}^{2} - m_{a}^{2})\varphi^{2}}{1 + \exp\left[-2C_{H}(\varphi^{2} - \varphi_{c}^{2})/M_{p}^{2}\right]} . \quad (25)$$

The parameter C_H depends on the smoothness of $b_{\min}(c)$ and thus on the potential of the \mathfrak{b} field. From now on we will treat it as a free parameter, but since no transition can be super-Planckian in string theory, we do not expect it to be larger than 1.

1. General details of the construction

Without the presence of fluxes in our theory there are massless fields corresponding to the complex structure moduli, dilaton modulus, and Kähler moduli. The tadpole condition is also not obeyed since D3-brane sources were included. We now propose a procedure à la KKLT [9, 44, 45] in order to stabilize the complex structure, dilaton, and Kähler moduli in a two-step procedure. We uplift the solution to a de Sitter solution as an extra final step. Namely, we propose to include suitable 3-form fluxes

in order to stabilize the complex structure z and dilaton moduli τ , and also meet the tadpole cancellation condition. Following that, we introduce non-perturbative corrections to stabilize all Kähler moduli, ρ , and all the others coming from cycles. It is not in the scope of this paper to work out these calculations in detail, but we wish to give a general view of our construction.

We want to include fluxes in our theory. The way these fluxes can be included in our compactified construction without influencing our background is by gluing a noncompact manifold to our compactified CY, similar to the simple mechanism done in [45], where the fluxes are included in a conifold of the CY manifold (an extension of the Klebanov-Strassler work for compact manifolds) [9]. We assume that the internal space is very large, in a way that supergravity is still valid, but with a size where the 4-dimensional Newton's constant is still finite (nonvanishing), and that the non-compact manifold is located far away from the warped region where our model is described. So, we include localized fluxes in the noncompact manifold far away from where we added our sources in the compactified manifold. We assume that there is no backreaction, which means that the fluxes are not coupled to the sources and that their influence dies off towards the direction of the D3-branes. In this way, the physics in the neighborhood of the D3-branes and the torsional cycles is essentially unchanged.

The presence of these localized 3-form fluxes in the non-compact manifold does not change locally what is happening where our theory lives. However, it changes globally the theory. The tadpole condition, or charge conservation, is a global condition. So, no matter where one localizes those fluxes, only the presence of fluxes with negative D3-brane charges is enough to ensure that the tadpole condition is met. The complex structure and dilaton moduli are stabilized by the presence of those fluxes. The fluxes generate a Gukov-Vafa-Witten (GVW) flux superpotential (W), which stabilizes the complex structure and dilaton moduli at a supersymmetric minimum of the potential, $D_{\tau}W = D_{z}W = 0$. So, the presence of fluxes fixes all of the complex structure and the dilaton moduli but leaves all the Kähler moduli unfixed. We need to tune those fluxes correctly in order to precisely obey the tadpole condition and control those moduli. Working out explicitly these solution is beyond the scope of this

Now, we have to stabilize the Kähler modulus [9, 44, 45]. This can be done by inducing a potential via a non-perturbative effect like gaugino condensation on a D7-brane or if the four-cycle Σ_4 is wrapped by D3-brane instantons, also called Euclidean D3-branes. By finding the minimum at $D_{\rho}W = 0$, the Kähler modulus is stabilized.

The vacuum found above has an AdS minimum with negative energy. Since we are interested in inflationary solutions, we need to uplifting the AdS minimum to a de Sitter vacuum. This can be done by any of the known mechanisms in the literature, for example [9, 44]. A differ-

ent approach can be found in [46]. The KKLT procedure is to add an uplifting potential to the theory, which breaks SUSY, and thus slightly shifts the minimum without disrupting the physics that led to the stabilized minimum. More details on this procedure can be seen in [9].

The above details give a broad view of how to realize our new axion monodromy model. The resolution of some of those topics is still unknown in the field, and these problems are present in many string inflation models. Those are material for deeper studies in axion monodromy and in general string inflation.

Also, in the present study, we have adopted a much simplified treatment of the warping effects in deriving the four-dimensional effective action. In the literature, there are a number of efforts on this subject, for example, see [36–42] for relevant extensive studies and [47, 48] for comprehensive reviews on the topic of flux compactification. Since the major focus of this paper is the cosmological implications of our model, we wish to leave more detailed studies of this aspect for future work.

III. INFLATIONARY DYNAMICS AND COSMOLOGICAL IMPLICATIONS

In this section, we select one specific model of the new axion monodromy model as a demonstration to study its cosmological implications. Specifically, we consider the effective action in (21) and assume a negligible Chern-Simons term. Then the Lagrangian derived at the end of the previous section can be rewritten as

$$\mathcal{L} = -\frac{1}{2}\partial_{\mu}\varphi\partial^{\mu}\varphi - V(\varphi) , \qquad (26)$$

which is viewed as an effective Lagrangian in 4-dimensional spacetime. The potential of the inflaton takes the form of $m_b^2 \varphi^2/2$ when $|\varphi| > \varphi_c$ (which corresponds to the UV regime) while taking the form of $m_a^2 \varphi^2/2$ when $|\varphi| \le \varphi_c$ (which belongs to the IR regime). We note that $m_b > m_a$ is required for the model to be consistent with theoretical constraints. For convenience, we would like to parameterize the potential in the following form,

$$V(\varphi) = \frac{1}{2}m_a^2 \varphi^2 + \frac{(m_b^2 - m_a^2)\varphi^2}{2\left\{1 + \exp\left[-2C_H(\varphi^2 - \varphi_c^2)/M_p^2\right]\right\}},$$
(27)

where we have introduced one dimensionless coefficient C_H in order to smoothly connect the UV and IR regimes of the potential near the critical scale characterized by φ_c . This newly introduced parameter ought to be determined by the explicit physics of the mass transition in the corresponding string theory construction. However, due to the lack of specific stringy derivations, we argue that C_H can be treated as a free parameter in our model that can be constrained by cosmological observations as will be analyzed in the following subsections.

We provide a sketch of the parameterized potential $V(\varphi)$ given by Eq. (27) in Fig. 1. This figure is helpful to gain a

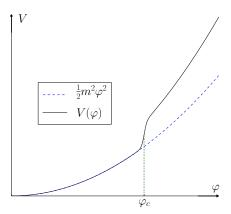


FIG. 1: Sketch of the potential V as a function of the inflation scalar field φ for our model (the solid black line) and for regular chaotic inflation (the dashed blue line). The potential under consideration takes the form of a quadratic function at both high and low energy scales, but there is a step-like profile that connects these two regimes at a critical scale φ_c . From the perspective of string theory, it indicates a vibration of the internal space. In our specific parametrization, we smooth out the step profile, the steepness of which is characterized by the dimensionless parameter C_H .

semi-analytic understanding of the background dynamics, which is the topic we turn to in the following subsection. We note that features in the inflationary potential such as above have a long history, namely see [49] for a pioneer study and [50, 51] for phenomenological constructions. Also, we note that a similarly featured potential was implemented phenomenologically by a model of multifield inflation in [52–54].

A. Background dynamics

In this subsection, we perform the detailed analysis of the background inflationary dynamics of the present model. It is well known that a model of φ^2 inflation possesses a local attractor solution regardless of the initial condition for the background scalar and that this is a slow-roll solution [55]. Accordingly, in both the UV and IR regimes of our model, the inflaton field can enter a period of slow-roll dynamics. Thus, in order to analyze the background dynamics semi-analytically, it is convenient to introduce a series of slow-roll parameters as follows,

$$\epsilon \equiv -\frac{\dot{H}}{H^2} , \quad \epsilon_{\varphi} \equiv \frac{M_p^2}{2} \left(\frac{V_{,\varphi}}{V}\right)^2 ,$$
(28)

$$\eta_{\varphi} \equiv M_p^2 \frac{V_{,\varphi\varphi}}{V} , \quad \xi_{\varphi} \equiv M_p^4 \frac{V_{,\varphi}V_{,\varphi\varphi\varphi}}{V^2} ,$$
(29)

where a dot denotes a derivative with respect to cosmic time (t) and where the subscript $_{,\varphi}$ denotes a derivative with respect to φ .

During inflation, the size of the universe is growing nearly exponentially while the Hubble rate is slowly varying. Thus, instead of cosmic time, it is very efficient

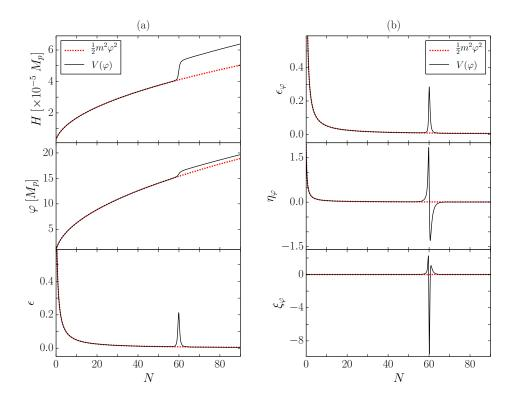


FIG. 2: Plots of the background parameters H, φ , and of the slow-roll parameters ϵ , ϵ_{φ} , η_{φ} , and ξ_{φ} in our model (solid black curves) and in regular quadratic inflation (dotted red curves). The horizontal axis represents the e-folding number N with N=0 being set by the condition $\epsilon(t_{\rm end})=1$, i.e. the end of inflation.

to apply the inflationary e-folding number to characterize the time duration of the process. Accordingly, the inflationary e-folding number is defined by

$$N(t) \equiv \int_{t}^{t_{\rm end}} H dt = \int_{\varphi_{\rm end}}^{\varphi} \frac{d\varphi}{\sqrt{2\epsilon} M_p} , \qquad (30)$$

where the end of inflation is determined by the condition $\epsilon(t_{\rm end}) = 1$.

When the single field φ evolves stably along the slow-roll trajectory, it is not difficult to observe that the value of ϵ approximately equals the value of ϵ_{φ} . One can easily derive the following approximate relations,

$$\epsilon_{\varphi} \simeq \eta_{\varphi} \simeq \frac{2M_p^2}{\varphi^2} \; , \; \xi_{\varphi} \simeq 0 \; ,$$
(31)

when the inflaton field is far away from the critical scale. When φ evolves near the critical value φ_c , the potential experiences a sudden decrease and its profile becomes very steep. In response to this change in the potential, ϵ and ϵ_{φ} can increase significantly before returning to their regular value after the critical phase. The slow-roll parameter $|\eta_{\varphi}|$ can also obtain a dramatic increase around the critical scale but the shape of the amplification is fairly asymmetric since this parameter characterizes the second derivative of the potential. It is interesting to note that $|\xi_{\varphi}|$ in standard quadratic inflation is always zero, but in

our model, it can become very large when the inflaton evolves through φ_c .

In the following, we numerically compute the background dynamics of our model. In Fig. 2, we plot the evolution of the Hubble rate H, the inflaton field φ , as well as the slow-roll parameters ϵ , ϵ_{φ} , η_{φ} , and ξ_{φ} with respect to the e-folding number N (solid black curves). Our model has four parameters, which are chosen to be, in Planck units,

$$m_a = 6.5175 \times 10^{-6} , \quad \varphi_c = 16 ,$$

 $m_b = 7.9433 \times 10^{-6} , \quad C_H = 0.1 ,$ (32)

for this specific example. In order to make a comparison, we also compute the background dynamics of quadratic inflation with a mass m_a (dotted red curves). We note that we set N=0 to be the end of inflation where $\epsilon(t_{\rm end})=1$. Thus, in these figures, inflation begins on the right where all the slow-roll parameters are small and proceeds to the left where both the Hubble rate and the inflaton field decrease to smaller values.

From the plots in Fig. 2, one can clearly see that the behavior of the slow-roll parameters is in agreement with the arguments given above. It is interesting to note that when the inflaton field approaches φ_c , its evolution presents a small step feature, and correspondingly, the Hubble rate experiences a sudden decrease at the same moment. Even though this variation is very small, it still

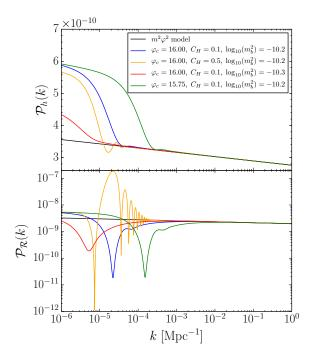


FIG. 3: Power spectrum for tensor modes (\mathcal{P}_h) and for curvature perturbations $(\mathcal{P}_{\mathcal{R}})$ as a function of the length scale of the perturbations in Fourier space (k). The black curve shows the power spectra for standard quadratic inflation where the mass of the inflaton is taken to be $m = m_a = 6.5175 \times 10^{-6}$. The colored curves show the power spectra for the model presented in this section with different parameter values.

leads to a series of changes in the slow-roll parameters. In particular, ξ_{φ} , which characterizes the third derivative of the potential with respect to φ , is vanishingly small for standard inflationary models. Here, we notice that it can be amplified up to $\mathcal{O}(10)$.

We can see from Fig. 2 that the deviations between our model and the regular $m^2\varphi^2$ model are still very small. Firstly, this is consistent with the nature of inflationary cosmology in which any deviation from the attractor solution damps out quickly. Secondly, even though these differences are very small, they can affect the process during which the primordial perturbation modes exit the Hubble radius near the pivot scale. We note that in our numerical computations, the pivot scale, which is taken to be $k_* = 0.002 \; {\rm Mpc}^{-1}$, corresponds to the e-folding number $N \simeq 55$. Accordingly, this can leave an imprint in the primordial power spectra. This is the subject that we explore in the following subsection.

B. Perturbation analysis

We already see from the previous section that, at the background level, a step-like feature in the potential induces a short period of time where the slow-roll conditions are violated. We therefore expect this to have implications in the perturbative regime. In fact, the near scaleinvariant power spectra typically obtained from quadratic inflation are likely to be modified, so in this section, we explore the quantitative consequences of the model introduced above.

The power spectra for metric perturbations are usually found by solving the Einstein field equations expanded about the background solution to linear order. For scalar modes, a gauge-invariant perturbation quantity is the curvature perturbation \mathcal{R} , and for tensor modes, it is the usual gravitational wave polarization state h (see [56] for a review of cosmological perturbations). The respective power spectra are then defined as $\mathcal{P}_{\mathcal{R}}(k) \equiv k^3 |\mathcal{R}_k|^2 / (2\pi^2)$ and $\mathcal{P}_h(k) \equiv k^3 |h_k|^2 / (2\pi^2)$. Given the complexity of the potential energy for the scalar field and of the background dynamics, we solve the perturbations equations for \mathcal{R} and h numerically in order to obtain their power spectra. More specifically, we use the recently developed MultiModeCode² [57-59]. This code is optimized for multi-field inflation, but its implementation makes it easy to evolve single field inflation with the potential defined in Eq. (27).

The resulting power spectra are shown in Fig. 3. We plotted the standard near scale-invariant power spectra for quadratic inflation in black, and the color curves show the modified potential with different parameter values. We first notice that for $k \gtrsim 10^{-2} \text{ Mpc}^{-1}$, the standard $m^2\varphi^2$ potential and the modified potential yield near identical power spectra. Moreover, for the parameter values shown in Fig. 3, our model predicts a similar tilt and tensor-to-scalar ratio compared to quadratic inflation with $n_s \approx 0.96$ and $r \approx 0.14$ at the pivot scale of $k_* =$ 0.05 Mpc⁻¹. It is only on larger length scales that the spectra deviate from near scale invariance due to the short phase of slow-roll violation during the inflationary period. Overall, the modified potential tends to lower the amplitude of the curvature perturbations and enhance the amount of gravitational waves produced. The effect is more radical when the drop in the potential depicted in Fig. 1 is very steep. In our parametrization of the potential, this is equivalent to having a large value of C_H . This is shown by the orange curve which has small damped non-harmonic oscillations for tensor modes but very large ones in the curvature power spectrum. However, such a large value for C_H is not expected from string theory (see Sec. IIB).

The effect is less drastic when the drop in the potential is smooth and this can be seen with the curves in red, blue, and green. In particular, the smallest effect is found when the large mass scale m_b is close to m_a (red curve). In this case, the jump in the potential is small and the feature in the power spectra occurs only in the far infrared. Finally, we note that changing the critical field value φ_c at which the jump in the potential occurs affects the scale at which the power spectra leave near scale-invariance.

² MultiModeCode web page: www.modecode.org.

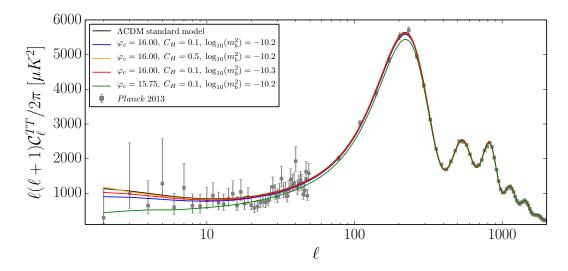


FIG. 4: Temperature (TT) angular power spectrum. The grey squares show the results of the *Planck* 2013 experiment and the black curve shows the standard Λ CDM model. The colored curves show the angular power spectrum for the model presented in this section with different parameter values. The value $m_a = 6.5175 \times 10^{-6}$ is fixed. The value of the cosmological parameters (e.g., $\Omega_b h^2$, $\Omega_c h^2$, H_0) are taken from the *Planck* 2013 collaboration and they are fixed at the same value for every curve. Furthermore, for the Λ CDM curve, the primordial power spectrum is parameterized by $\mathcal{P}_{\mathcal{R}}(k) = A_s(k/k_*)^{n_s-1}$ where we take $A_s = 2.21536 \times 10^{-9}$, $k_* = 0.05$ Mpc⁻¹, and $n_s = 0.96$.

More specifically, the lower the energy scale of the drop in the potential, the lower the length scale of the feature in the power spectra.

Let us provide some further physical intuition for the above description of the power spectra. The small kmodes (large wavelength) exit the Hubble radius at early times when the inflaton is in its first slow-roll phase, i.e. when the potential looks like $m_b^2 \varphi^2/2$. At this point, the power spectra are given by their usual forms [60] with an amplitude proportional to $H^2/(\epsilon M_p^2)$ for curvature perturbations and proportional to H^2/M_p^2 for tensor modes. Thus, the amplitudes depend on m_b^2 (the larger mass scale). Similarly, the large k modes (small wavelength) exit the Hubble radius at late times when the inflaton is in its second slow-roll phase, i.e. when the potential looks like $m_a^2 \varphi^2/2$, so the amplitude of the spectra depends on m_a^2 (the smaller mass scale). In particular, the amplitude of the spectra at the pivot scale $k_* = 0.05 \text{ Mpc}^{-1}$ is most sensitive to the mass parameter m_a . Finally, modes of intermediate wavelengths exit the Hubble radius near the critical scale φ_c at which point the slow-roll conditions are violated. Consequently, the power spectra do not follow their usual near scale-invariance for slow-roll inflation. The behavior of the power spectra in this regime depends on the parameter values of the model and has been described for a number of cases in the previous paragraph.

To further connect with observations, we evolve the resulting power spectra after inflation to the angular power spectra that can be probed observationally at the time of the CMB with telescopes such as *Planck*. To do this,

we use $CAMB^3$ [61] where we input our power spectrum for curvature perturbations and tensor modes as shown in Fig. 3 instead of a parameterized power spectrum as it is usually done for the standard ΛCDM model. Furthermore, we use the best fit to the cosmological parameters found by Planck [1] in the code.

First, the temperature (TT) angular power spectrum is shown in Fig. 4. The grey squares show the measured data by Planck~2013 and the black curve shows the standard ΛCDM curve for a parameterized power spectrum after inflation. The color curves show the angular power spectrum for the modified potential, and similar to our conclusion from the power spectra after inflation, the different angular power spectra are very similar on small scales ($\ell \gtrsim 300$).

The differences with Λ CDM are more distinct around the first acoustic peak and at low ℓ 's. In particular, we notice that the amplitude of the green curve is much smaller than the other ones for $\ell \lesssim 300$. This was expected from the fact that the curvature power spectrum for the green curve is the one that deviates from near scale-invariance at the smallest scale (see lower panel of Fig. 3) since it has the smallest φ_c . Although the low amplitude of the angular power spectrum around the first acoustic peak may imply larger differences in the cosmological parameters compared to the Planck 2013 results, the green curve has the advantage of explaining the low- ℓ suppression of the spectrum. Such a suppression is also obtained in the case of the blue and red curves, although

³ CAMB web page: http://camb.info.

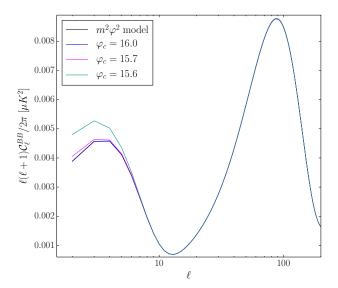


FIG. 5: Unlensed B-mode polarization angular power spectrum. The black curve shows the standard result for quadratic inflation. The blue, magenta, and turquoise curves show the result for our model when the critical scale φ_c changes. The other parameters are kept fixed: $m_a = 6.5175 \times 10^{-6}$, $m_b = 7.9433 \times 10^{-6}$, $C_H = 0.1$. We note that the black curve is completely hidden below the blue curve.

at a smaller extent than for the case of the green curve, but these curves have the advantage of closely matching Λ CDM around the first acoustic peak. To summarize, the larger the k-mode at which the feature appears in the curvature power spectrum, the larger the deviation from Λ CDM, but the larger the low- ℓ suppression is.

The situation is somewhat different for the orange curve in the case of a steep drop in the potential (large C_H). Indeed, this case follows ΛCDM very closely at all angular scales except at $\ell=2$ where the amplitude for the modified potential is larger and this seems to be in greater conflict with the observation. This reinforces our intuition that a steep drop in the potential is not favored.

Second, we show the unlensed B-mode polarization angular power spectrum in Fig. 5, i.e. the primordial contribution to the total B-mode power spectrum. The figure shows that the axion monodromy model with different parameter values agrees with the quadratic potential at almost all angular scales. In fact, for $\ell \gtrsim 7$, the spectra are basically identical. This is in agreement with the top panel of Fig. 3 which showed very similar tensor power spectra for large k.

It is only at very large angular scales ($\ell \lesssim 7$) that one can notice a small deviation. This deviation is only significant when the critical scale φ_c is small since this is when the deviation from near scale invariance in the primordial power spectrum occurs at larger k. We notice that the amplification at small ℓ in the BB power spectrum is very small compared to the suppression in the TT power spectrum. This is in accordance with the power spectra after inflation shown in Fig. 3 where the suppression in

 $\mathcal{P}_{\mathcal{R}}$ can be of more than one order of magnitude, whereas the amplification in \mathcal{P}_h is only of order one. Clearly, the suppression in the TT spectrum and the amplification in the BB spectrum are correlated, so one needs to compare both spectra with observations to constrain the model. Still, the amplification at large angular scales in the BB spectrum is an interesting feature of this model and one hopes to explore this region as well as the entire spectrum with future CMB polarization data.

C. Fitting to cosmological data

After analyzing the temperature angular power spectrum, one would hope to be able to determine which model best fits the observed data. In Fig. 4, the cosmological parameters are fixed, but when one allows them to be free, it is possible to fit all the cosmological parameters to the data given the model that is studied. This is what we explore with Markov Chain Monte Carlo (MCMC) simulations.

We perform a model comparison with CosmoMC⁴ [62] by running the MCMC code for the red, blue, and green curves of Fig. 4. The usual cosmological parameters (except the ones related to a parameterized power spectrum such as n_s and A_s , which are ignored) are given the same prior range as *Planck* [1]. The runs reached convergency as we can see from the Gelman-Rubin statistic R-1 value [63, 64] of 0.01325, 0.01276, and 0.01103 in the case of the red, blue, and green curves, respectively. The resulting likelihoods can then be compared to determine which of the three cases best fits the *Planck* 2013 data, but we find that the likelihoods are all identical within the precision of the results. Furthermore, running the action 2 from CosmoMC leads to the same conclusion: the respective χ^2 are near identical and it is therefore not possible to tell which case is best.

For this reason, we leave model comparison aside and simply compare the CosmoMC results for our model with the standard Λ CDM model from *Planck* 2013. In Fig. 6, we show constraints on pairs of cosmological parameters and their respective probability distributions for the CosmoMC runs described above and for the results from Planck 2013. We first notice that the colored curve which represent our model are almost perfectly superposed, in agreement with our likelihood analysis. Also, we notice that the resulting best fits to the cosmological parameters are all very close to one another even when comparing with the Planck 2013 results. They differ by fractions of the order of 1% at most. This suggests that the model tested here is in good agreement with the observations. We stress though that the above analysis cannot indicate which of the axion monodromy model and the standard model is best. Indeed, the standard model assumes a parameter-

⁴ CosmoMC web page: http://cosmologist.info/cosmomc.

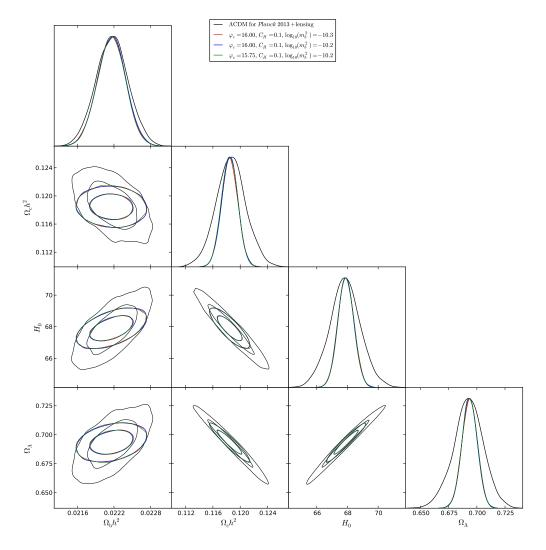


FIG. 6: Constraints on pairs of cosmological parameters (1σ and 2σ contour lines) and probability distributions for the baryon density today ($\Omega_b h^2$), the cold dark matter density today ($\Omega_c h^2$), the Hubble parameter today (H_0), and the dark energy density divided by the critical density today (Ω_{Λ}). The color scheme is the same as for Fig. 4.

ized power spectrum of the form $\mathcal{P}_{\mathcal{R}}(k) = A_s(k/k_*)^{n_s-1}$ and thus fits two additional parameters, i.e. A_s and n_s . This in part explains why the cosmological parameters in Fig. 6 are better constrained by our model than by the standard model and why more correlation seems present (especially for $\Omega_b h^2$) in the standard model than in the axion monodromy model.

IV. CONCLUSIONS

In the present paper, we proposed a new model of axion monodromy inflation. Analogously to regular models of axion monodromy inflation in which the effective theory is derived from the reduction of a higher dimensional theory on a two-cycle, our model is constructed in the presence of torsional cycles. In particular, our model possesses at least three scalar fields that can be candidates for the inflaton. Amongst them, two fields are free of the η problem due to

mass corrections of the moduli stabilization in the Kähler potential, and hence, the theory is well established from the perspective of string theory.

As a particular realization of this model, we studied quadratic inflation where the potential is effectively transformed to have two mass scales separated by a step-like feature at some critical scale. At the background level, one finds a short phase in which the slow-roll conditions are violated. Perturbatively, the power spectrum of curvature perturbations is either suppressed or oscillates near the critical scale depending on the details of the potential, and the power spectrum of tensor modes is boosted on large scales.

In light of recent and forthcoming CMB experiments, a lot of analyses have aimed at searching for features of inflation or its alternatives (see, e.g., [53, 54, 65–89] for extensive discussions). In our model, we have two interesting predictions: one is that there exits a moderate boost in the CMB B-mode polarization spectrum at small

 ℓ 's; the other is a defect of temperature anisotropies in the same regime, which provides a natural interpretation for the low- ℓ suppression anomaly in the CMB data. It will be interesting to perform a full global fitting analysis with the *Planck* 2015 data to confront these predictions with cosmological observations, which will be presented in a follow-up letter [90].

We point out that while this paper was being prepared for submission, the preprint of [91] appeared, which explores features of standard axion monodromy inflation with drifting oscillations.

Acknowledgments

We thank Robert Brandenberger, Jim Cline, Gil Holder, Bin Hu, Gary Shiu, Gabrielle Simard, Anzhong Wang, and in particular, Keshav Dasgupta, Evan McDonough, and Gim Seng Ng for valuable discussions. YFC is supported in part by the Natural Sciences and Engineering Research Council (NSERC) of Canada, by the Department of Physics at McGill University, by the Chinese National Youth Thousand Talents Program, by the USTC start-up funding (KY2030000049), and by the Natural Science Foundation of China (Grant No. 11421303). FC is supported by National Science Foundation (NSF) Grant No. PHY11-25915. EF thanks CNPa (Science without Borders) for financial support. JQ acknowledges the support, throughout the completion of this work, of the Fonds de recherche du Québec - Nature et technologies (FRQNT), the Walter C. Sumner Foundation, and NSERC via the Vanier Canada Graduate Scholarships program. Computations were made on the supercomputer Guillimin from McGill University, managed by Calcul Québec and Compute Canada. The operation of this supercomputer is funded by the Canada Foundation for Innovation (CFI), NanoQuébec, RMGA and FRQNT.

- P. A. R. Ade et al. [Planck Collaboration], "Planck 2013 results. XVI. Cosmological parameters," Astron. Astrophys. 571, A16 (2014) [arXiv:1303.5076 [astro-ph.CO]].
- [2] P. A. R. Ade et al. [Planck Collaboration], "Planck 2013 results. XXII. Constraints on inflation," Astron. Astrophys. 571, A22 (2014) [arXiv:1303.5082 [astro-ph.CO]].
- [3] P. A. R. Ade et al. [BICEP2 Collaboration], "Detection of B-Mode Polarization at Degree Angular Scales by BICEP2," Phys. Rev. Lett. 112, 241101 (2014) [arXiv:1403.3985 [astro-ph.CO]].
- [4] D. H. Lyth, "What would we learn by detecting a gravitational wave signal in the cosmic microwave background anisotropy?," Phys. Rev. Lett. 78, 1861 (1997) [hep-ph/9606387].
- [5] M. J. Mortonson and U. Seljak, "A joint analysis of Planck and BICEP2 B modes including dust polarization uncertainty," JCAP 1410, no. 10, 035 (2014) [arXiv:1405.5857 [astro-ph.CO]].
- [6] R. Flauger, J. C. Hill and D. N. Spergel, "Toward an Understanding of Foreground Emission in the BICEP2 Region," JCAP 1408, 039 (2014) [arXiv:1405.7351 [astro-ph.CO]].
- [7] R. Adam et al. [Planck Collaboration], "Planck intermediate results. XXX. The angular power spectrum of polarized dust emission at intermediate and high Galactic latitudes," Astron. Astrophys. 586, A133 (2016) [arXiv:1409.5738 [astro-ph.CO]].
- [8] C. P. Burgess, M. Cicoli and F. Quevedo, "String Inflation After Planck 2013," JCAP 1311, 003 (2013) [arXiv:1306.3512 [hep-th]].
- [9] D. Baumann and L. McAllister, "Inflation and String Theory," arXiv:1404.2601 [hep-th].
- [10] A. Westphal, "String cosmology Large-field inflation in string theory," Int. J. Mod. Phys. A 30, no. 09, 1530024 (2015) [arXiv:1409.5350 [hep-th]].
- [11] E. Silverstein and A. Westphal, "Monodromy in the CMB: Gravity Waves and String Inflation," Phys. Rev. D 78, 106003 (2008) [arXiv:0803.3085 [hep-th]].

- [12] L. McAllister, E. Silverstein and A. Westphal, "Gravity Waves and Linear Inflation from Axion Monodromy," Phys. Rev. D 82, 046003 (2010) [arXiv:0808.0706 [hep-th]].
- [13] R. Flauger, L. McAllister, E. Pajer, A. Westphal and G. Xu, "Oscillations in the CMB from Axion Monodromy Inflation," JCAP 1006, 009 (2010) [arXiv:0907.2916 [hep-th]].
- [14] L. McAllister, E. Silverstein, A. Westphal and T. Wrase, "The Powers of Monodromy," JHEP 1409, 123 (2014) [arXiv:1405.3652 [hep-th]].
- [15] F. Marchesano, G. Shiu and A. M. Uranga, "F-term Axion Monodromy Inflation," JHEP 1409, 184 (2014) [arXiv:1404.3040 [hep-th]].
- [16] R. Blumenhagen and E. Plauschinn, "Towards Universal Axion Inflation and Reheating in String Theory," Phys. Lett. B 736, 482 (2014) [arXiv:1404.3542 [hep-th]].
- [17] A. Hebecker, S. C. Kraus and L. T. Witkowski, "D7-Brane Chaotic Inflation," Phys. Lett. B 737, 16 (2014) [arXiv:1404.3711 [hep-th]].
- [18] L. E. Ibáñez and I. Valenzuela, "The inflaton as an MSSM Higgs and open string modulus monodromy inflation," Phys. Lett. B 736, 226 (2014) [arXiv:1404.5235 [hep-th]].
- [19] S. Franco, D. Galloni, A. Retolaza and A. Uranga, "On axion monodromy inflation in warped throats," JHEP 1502, 086 (2015) [arXiv:1405.7044 [hep-th]].
- [20] K. Freese, J. A. Frieman and A. V. Olinto, "Natural inflation with pseudo - Nambu-Goldstone bosons," Phys. Rev. Lett. 65, 3233 (1990).
- [21] J. E. Kim, H. P. Nilles and M. Peloso, "Completing natural inflation," JCAP 0501, 005 (2005) [hep-ph/0409138].
- [22] R. Kappl, S. Krippendorf and H. P. Nilles, "Aligned Natural Inflation: Monodromies of two Axions," Phys. Lett. B 737, 124 (2014) [arXiv:1404.7127 [hep-th]].
- [23] C. Long, L. McAllister and P. McGuirk, "Aligned Natural Inflation in String Theory," Phys. Rev. D 90, 023501 (2014) [arXiv:1404.7852 [hep-th]].
- [24] T. C. Bachlechner, M. Dias, J. Frazer and L. McAllister,

- "Chaotic inflation with kinetic alignment of axion fields," Phys. Rev. D **91**, no. 2, 023520 (2015) [arXiv:1404.7496 [hep-th]].
- [25] R. Blumenhagen, D. Herschmann and E. Plauschinn, "The Challenge of Realizing F-term Axion Monodromy Inflation in String Theory," JHEP 1501, 007 (2015) [arXiv:1409.7075 [hep-th]].
- [26] H. Hayashi, R. Matsuda and T. Watari, "Issues in Complex Structure Moduli Inflation," arXiv:1410.7522 [hepth].
- [27] A. Hebecker, P. Mangat, F. Rompineve and L. T. Witkowski, "Tuning and Backreaction in Fterm Axion Monodromy Inflation," Nucl. Phys. B 894, 456 (2015) [arXiv:1411.2032 [hep-th]].
- [28] M. Berg, E. Pajer and S. Sjors, "Dante's Inferno," Phys. Rev. D 81, 103535 (2010) [arXiv:0912.1341 [hep-th]].
- [29] S. Hannestad, T. Haugbolle, P. R. Jarnhus and M. S. Sloth, "Non-Gaussianity from Axion Monodromy Inflation," JCAP 1006, 001 (2010) [arXiv:0912.3527 [hep-ph]].
- [30] J. P. Conlon, "Brane-Antibrane Backreaction in Axion Monodromy Inflation," JCAP 1201, 033 (2012) [arXiv:1110.6454 [hep-th]].
- [31] B. Shlaer, "Chaotic Brane Inflation," Phys. Rev. D 88, 103503 (2013) [arXiv:1211.4024 [hep-th]].
- [32] X. Gao, T. Li and P. Shukla, "Combining Universal and Odd RR Axions for Aligned Natural Inflation," JCAP 1410, no. 10, 048 (2014) [arXiv:1406.0341 [hep-th]].
- [33] O. Özsoy, K. Sinha and S. Watson, "How Well Can We Really Determine the Scale of Inflation?," Phys. Rev. D 91, no. 10, 103509 (2015) [arXiv:1410.0016 [hep-th]].
- [34] N. Kaloper and L. Sorbo, "A Natural Framework for Chaotic Inflation," Phys. Rev. Lett. 102, 121301 (2009) [arXiv:0811.1989 [hep-th]].
- [35] E. J. Copeland, A. R. Liddle, D. H. Lyth, E. D. Stewart and D. Wands, "False vacuum inflation with Einstein gravity," Phys. Rev. D 49, 6410 (1994) [astro-ph/9401011].
- [36] O. DeWolfe and S. B. Giddings, "Scales and hierarchies in warped compactifications and brane worlds," Phys. Rev. D 67, 066008 (2003) [hep-th/0208123].
- [37] S. P. de Alwis, "On Potentials from fluxes," Phys. Rev. D 68, 126001 (2003) [hep-th/0307084].
- [38] S. B. Giddings and A. Maharana, "Dynamics of warped compactifications and the shape of the warped landscape," Phys. Rev. D 73, 126003 (2006) [hep-th/0507158].
- [39] G. Shiu, G. Torroba, B. Underwood and M. R. Douglas, "Dynamics of Warped Flux Compactifications," JHEP 0806, 024 (2008) [arXiv:0803.3068 [hep-th]].
- [40] M. R. Douglas and G. Torroba, "Kinetic terms in warped compactifications," JHEP 0905, 013 (2009) [arXiv:0805.3700 [hep-th]].
- [41] A. R. Frey, G. Torroba, B. Underwood and M. R. Douglas, "The Universal Kahler Modulus in Warped Compactifications," JHEP 0901, 036 (2009) [arXiv:0810.5768 [hep-th]].
- [42] B. Underwood, "A Breathing Mode for Warped Compactifications," Class. Quant. Grav. 28, 195013 (2011) [arXiv:1009.4200 [hep-th]].
- [43] L. Anguelova, C. Quigley and S. Sethi, "The Leading Quantum Corrections to Stringy Kahler Potentials," JHEP 1010, 065 (2010) [arXiv:1007.4793 [hep-th]].
- [44] S. Kachru, R. Kallosh, A. D. Linde and S. P. Trivedi, "De Sitter vacua in string theory," Phys. Rev. D 68, 046005

- (2003) [hep-th/0301240].
- [45] S. B. Giddings, S. Kachru and J. Polchinski, "Hierarchies from fluxes in string compactifications," Phys. Rev. D 66, 106006 (2002) [hep-th/0105097].
- [46] K. Dasgupta, R. Gwyn, E. McDonough, M. Mia and R. Tatar, "de Sitter Vacua in Type IIB String Theory: Classical Solutions and Quantum Corrections," JHEP 1407, 054 (2014) [arXiv:1402.5112 [hep-th]].
- [47] M. R. Douglas and S. Kachru, "Flux compactification," Rev. Mod. Phys. 79, 733 (2007) [hep-th/0610102].
- [48] F. Denef, M. R. Douglas and S. Kachru, "Physics of String Flux Compactifications," Ann. Rev. Nucl. Part. Sci. 57, 119 (2007) [hep-th/0701050].
- [49] A. A. Starobinsky, "Spectrum of adiabatic perturbations in the universe when there are singularities in the inflation potential," JETP Lett. 55, 489 (1992) [Pisma Zh. Eksp. Teor. Fiz. 55, 477 (1992)].
- [50] J. A. Adams, G. G. Ross and S. Sarkar, "Multiple inflation," Nucl. Phys. B 503, 405 (1997) [hep-ph/9704286].
- [51] J. A. Adams, B. Cresswell and R. Easther, "Inflationary perturbations from a potential with a step," Phys. Rev. D 64, 123514 (2001) [astro-ph/0102236].
- [52] B. Feng and X. Zhang, "Double inflation and the low cmb quadrupole," Phys. Lett. B 570, 145 (2003) [astroph/0305020].
- [53] M. Joy, V. Sahni and A. A. Starobinsky, "A New Universal Local Feature in the Inflationary Perturbation Spectrum," Phys. Rev. D 77, 023514 (2008) [arXiv:0711.1585 [astro-ph]].
- [54] M. Joy, A. Shafieloo, V. Sahni and A. A. Starobinsky, "Is a step in the primordial spectral index favored by CMB data?," JCAP 0906, 028 (2009) [arXiv:0807.3334 [astro-ph]].
- [55] J. H. Kung and R. H. Brandenberger, "Chaotic Inflation as an Attractor in Initial Condition Space," Phys. Rev. D 42, 1008 (1990).
- [56] R. H. Brandenberger, "Lectures on the theory of cosmological perturbations," Lect. Notes Phys. 646, 127 (2004) [hep-th/0306071].
- [57] M. J. Mortonson, H. V. Peiris and R. Easther, "Bayesian Analysis of Inflation: Parameter Estimation for Single Field Models," Phys. Rev. D 83, 043505 (2011) [arXiv:1007.4205 [astro-ph.CO]].
- [58] R. Easther and H. V. Peiris, "Bayesian Analysis of Inflation II: Model Selection and Constraints on Reheating," Phys. Rev. D 85, 103533 (2012) [arXiv:1112.0326 [astro-ph.CO]].
- [59] L. C. Price, J. Frazer, J. Xu, H. V. Peiris and R. Easther, "MultiModeCode: An efficient numerical solver for multifield inflation," JCAP 1503, no. 03, 005 (2015) [arXiv:1410.0685 [astro-ph.CO]].
- [60] V. F. Mukhanov, H. A. Feldman and R. H. Brandenberger, "Theory of cosmological perturbations. Part 1. Classical perturbations. Part 2. Quantum theory of perturbations. Part 3. Extensions," Phys. Rept. 215, 203 (1992).
- [61] A. Lewis, A. Challinor and A. Lasenby, "Efficient computation of CMB anisotropies in closed FRW models," Astrophys. J. 538, 473 (2000) [astro-ph/9911177].
- [62] A. Lewis and S. Bridle, "Cosmological parameters from CMB and other data: A Monte Carlo approach," Phys. Rev. D 66, 103511 (2002) [astro-ph/0205436].
- [63] A. Gelman and D. B. Rubin, "Inference from Iterative Simulation Using Multiple Sequences," Statist. Sci. 7, 457 (1992).

- [64] A. Lewis, "Efficient sampling of fast and slow cosmological parameters," Phys. Rev. D 87, no. 10, 103529 (2013) [arXiv:1304.4473 [astro-ph.CO]].
- [65] C. R. Contaldi, M. Peloso and L. Sorbo, "Suppressing the impact of a high tensor-to-scalar ratio on the temperature anisotropies," JCAP 1407, 014 (2014) [arXiv:1403.4596 [astro-ph.CO]].
- [66] A. Ashoorioon, K. Dimopoulos, M. M. Sheikh-Jabbari and G. Shiu, "Non-Bunch-Davis initial state reconciles chaotic models with BICEP and Planck," Phys. Lett. B 737, 98 (2014) [arXiv:1403.6099 [hep-th]].
- [67] B. Feng, M. Li, R. J. Zhang and X. Zhang, "An inflation model with large variations in spectral index," Phys. Rev. D 68, 103511 (2003) [astro-ph/0302479].
- [68] Y. Wan, S. Li, M. Li, T. Qiu, Y. Cai and X. Zhang, "Single field inflation with modulated potential in light of the Planck and BICEP2," Phys. Rev. D 90, 023537 (2014) [arXiv:1405.2784 [astro-ph.CO]].
- [69] V. Miranda, W. Hu and P. Adshead, "Steps to Reconcile Inflationary Tensor and Scalar Spectra," Phys. Rev. D 89, no. 10, 101302 (2014) [arXiv:1403.5231 [astro-ph.CO]].
- [70] H. Firouzjahi and M. H. Namjoo, "Jump in fluid properties of inflationary universe to reconcile scalar and tensor spectra," Phys. Rev. D 90, 063525 (2014) [arXiv:1404.2589 [astro-ph.CO]].
- [71] Y. S. Piao, B. Feng and X. m. Zhang, "Suppressing CMB quadrupole with a bounce from contracting phase to inflation," Phys. Rev. D 69, 103520 (2004) [hep-th/0310206];
- [72] J. Q. Xia, Y. F. Cai, H. Li and X. Zhang, "Evidence for bouncing evolution before inflation after BICEP2," Phys. Rev. Lett. 112, 251301 (2014) [arXiv:1403.7623 [astro-ph.CO]].
- [73] Y. F. Cai and Y. Wang, "Testing quantum gravity effects with latest CMB observations," Phys. Lett. B 735, 108 (2014) [arXiv:1404.6672 [astro-ph.CO]].
- [74] Y. F. Cai, "Exploring Bouncing Cosmologies with Cosmological Surveys," Sci. China Phys. Mech. Astron. 57, 1414 (2014) [arXiv:1405.1369 [hep-th]].
- [75] J. Hamann, L. Covi, A. Melchiorri and A. Slosar, "New Constraints on Oscillations in the Primordial Spectrum of Inflationary Perturbations," Phys. Rev. D 76, 023503 (2007) [astro-ph/0701380].
- [76] R. K. Jain, P. Chingangbam, J. O. Gong, L. Sri-ramkumar and T. Souradeep, "Punctuated inflation and the low CMB multipoles," JCAP 0901, 009 (2009) [arXiv:0809.3915 [astro-ph]].
- [77] R. K. Jain, P. Chingangbam, L. Sriramkumar and T. Souradeep, "The tensor-to-scalar ratio in punctuated inflation," Phys. Rev. D 82, 023509 (2010) [arXiv:0904.2518 [astro-ph.CO]].
- [78] M. J. Mortonson, C. Dvorkin, H. V. Peiris and W. Hu,

- "CMB polarization features from inflation versus reionization," Phys. Rev. D **79**, 103519 (2009) [arXiv:0903.4920 [astro-ph.CO]].
- [79] D. K. Hazra, M. Aich, R. K. Jain, L. Sriramkumar and T. Souradeep, "Primordial features due to a step in the inflaton potential," JCAP 1010, 008 (2010) [arXiv:1005.2175 [astro-ph.CO]].
- [80] D. K. Hazra, A. Shafieloo, G. F. Smoot and A. A. Starobinsky, "Inflation with Whip-Shaped Suppressed Scalar Power Spectra," Phys. Rev. Lett. 113, no. 7, 071301 (2014) [arXiv:1404.0360 [astro-ph.CO]].
- [81] D. K. Hazra, A. Shafieloo, G. F. Smoot and A. A. Starobinsky, "Wiggly Whipped Inflation," JCAP 1408, 048 (2014) [arXiv:1405.2012 [astro-ph.CO]].
- [82] D. K. Hazra, A. Shafieloo and G. F. Smoot, "Reconstruction of broad features in the primordial spectrum and inflaton potential from Planck," JCAP 1312, 035 (2013) [arXiv:1310.3038 [astro-ph.CO]].
- [83] K. N. Abazajian, G. Aslanyan, R. Easther and L. C. Price, "The Knotted Sky II: Does BICEP2 require a nontrivial primordial power spectrum?," JCAP 1408, 053 (2014) [arXiv:1403.5922 [astro-ph.CO]].
- [84] B. Hu, J. W. Hu, Z. K. Guo and R. G. Cai, "Reconstruction of the primordial power spectra with Planck and BI-CEP2," Phys. Rev. D 90, 023544 (2014) [arXiv:1404.3690 [astro-ph.CO]].
- [85] A. Ashoorioon and A. Krause, "Power Spectrum and Signatures for Cascade Inflation," hep-th/0607001.
- [86] A. Ashoorioon, A. Krause and K. Turzynski, "Energy Transfer in Multi Field Inflation and Cosmological Perturbations," JCAP 0902, 014 (2009) [arXiv:0810.4660 [hep-th]].
- [87] A. Ashoorioon, C. van de Bruck, P. Millington and S. Vu, "Effect of transitions in the Planck mass during inflation on primordial power spectra," Phys. Rev. D 90, no. 10, 103515 (2014) [arXiv:1406.5466 [astro-ph.CO]].
- [88] G. Ballesteros and J. A. Casas, "Large tensor-to-scalar ratio and running of the scalar spectral index with Instep Inflation," Phys. Rev. D 91, 043502 (2015) [arXiv:1406.3342 [astro-ph.CO]].
- [89] Y. Cai, Y. T. Wang and Y. S. Piao, "Oscillating modulation to B-mode polarization from varying propagating speed of primordial gravitational waves," Phys. Rev. D 91, 103001 (2015) [arXiv:1501.06345 [astro-ph.CO]].
- [90] Y. F. Cai, E. G. M. Ferreira, B. Hu and J. Quintin, "Searching for features of a string-inspired inflationary model with cosmological observations," Phys. Rev. D 92, no. 12, 121303 (2015) [arXiv:1507.05619 [astro-ph.CO]].
- [91] R. Flauger, L. McAllister, E. Silverstein and A. Westphal, "Drifting Oscillations in Axion Monodromy," arXiv:1412.1814 [hep-th].